# Carboxylate-Free $Mn^{III}_2Ln^{III}_2$ (Ln = Lanthanide) and $Mn^{III}_2Y^{III}_2$ Complexes from the Use of (2-Hydroxymethyl)pyridine: Analysis of Spin Frustration Effects

Constantina Papatriantafyllopoulou, Khalil A. Abboud, and George Christou*

Department of Chemistry, University of Florida, Gainesville, Florida 32611-7200, United States

Ⓢ *Supporting Information*

**ABSTRACT:** The initial employment of 2-(hydroxymethyl)pyridine for the synthesis of Mn/Ln (Ln = lanthanide) and Mn/Y clusters, in the absence of an ancillary organic ligand, has afforded a family of tetranuclear $[Mn^{III}_2M^{III}_2$-$(OH)_2(NO_3)_4(hmp)_4(H_2O)_4](NO_3)_2$ (M = Dy, **1**; Tb, **2**; Gd, **3**; Y, **4**) anionic compounds. **1−4** possess a planar butterfly (or rhombus) core and are rare examples of carboxylate-free Mn/Ln and Mn/Y clusters. Variable-temperature dc and ac studies established that **1** and **2**, which contain highly anisotropic $Ln^{III}$ atoms, exhibit slow relaxation of their magnetization vector. Fitting of the obtained magnetization ($M$) versus field ($H$) and temperature ($T$) data for **3** by matrix diagonalization and including only axial anisotropy (zero-field splitting, ZFS) showed the ground state to be $S = 3$. Complex **4** has an $S = 0$ ground state. Fitting of the magnetic susceptibility data collected in the 5−300 K range for **3** and **4** to the appropriate van Vleck equations revealed, as expected, extremely weak antiferromagnetic interactions between the paramagnetic ions; for **3**, $J_1 = -0.16(2)$ $cm^{-1}$ and $J_2 = -0.12(1)$ $cm^{-1}$ for the $Mn^{III}\cdots Mn^{III}$ and $Mn^{III}\cdots Gd^{III}$ interactions, respectively. The $S = 3$ ground state of **3** has been rationalized on the basis of the spin frustration pattern in the molecule. For **4**, $J = -0.75(3)$ $cm^{-1}$ for the $Mn^{III}\cdots Mn^{III}$ interaction. Spin frustration effects in **3** have been quantitatively analyzed for all possible combinations of sign of $J_1$ and $J_2$.
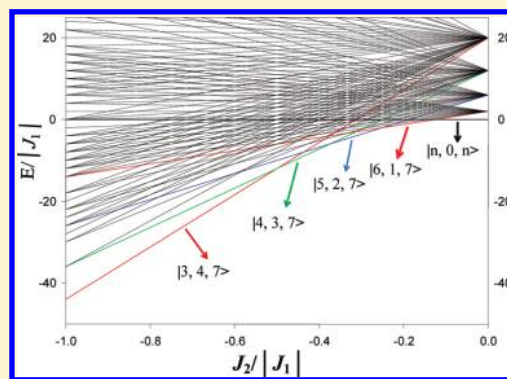


## ■ INTRODUCTION

Mixed 3d/4f metal cluster chemistry has been attracting intense interest during the last several years. There are many different reasons for this, including the aesthetically pleasing structures that many such molecular clusters possess, but the main reason is their relevance to nanoscale magnetic materials. Thus, polynuclear 3d/4f complexes have been investigated in the field of molecule-based magnets and single-molecule magnets (SMMs) as an alternative to homometallic transition metal compounds.[1] SMMs are individual molecules that can function as nanoscale magnetic particles below a blocking temperature and represent a molecular approach to nanomagnetism. The magnetic behavior of SMMs results from the combination of a large ground spin state ($S$) with a large and negative Ising (easy-axis) type of magnetoanisotropy, as measured by the axial zero-field splitting parameter, $D$. Most trivalent lanthanides possess large single-ion anisotropy, and the strategy has been to take advantage of this to target 3d/4f SMMs distinctly different from the homometallic 3d ones. Indeed, the first 3d/4f SMM was a $Cu_2Tb_2$ complex in 2004,[2] and the first Mn/Ln SMM was a $Mn_6Dy_6$ complex in the same year,[3] both exhibiting out-of-phase ac magnetic susceptibility signals. Also in 2004 were reported $Mn_{11}Ln_4$ SMMs,[4] the initial examples of 3d/4f SMMs exhibiting hysteresis and QTM.[5] Many other Mn/Ln SMMs have subsequently been reported, including $Mn_{21}Dy$,[6a] $Mn_{12}Gd$,[6b] $Mn_{11}Gd_2$,[7a]

$Mn_5Ln_4$,[7b] and $Mn_9Dy_8$.[7c] Only in a few cases have these species been amenable to elucidation of the magnitudes of their intramolecular exchange interactions and a resulting rationalization of how these lead to the observed ground state $S$ value. The reasons for this include (i) the often high nuclearity of these molecules and the consequently large number of pairwise exchange interactions ($J_{ij}$) present, many of which are competing and lead to spin frustration effects, (ii) the weak nature of the Mn—Ln and Ln—Ln exchange interactions due to the nature of the 4f orbitals, and (iii) spin—orbit coupling effects, which complicate magnetic susceptibility fits for polynuclear systems.[8] We have thus been on the lookout for additional examples of smaller Mn/Ln complexes for such analyses.

Several synthetic strategies have been employed by molecular chemists in the search for new structural types of Mn/Ln complexes. Such strategies usually rely on the use of small flexible ligands such as carboxylates ($RCO_2^-$). As a result, reactions in the absence of carboxylates have been poorly explored as a route to mixed Mn/Ln complexes.[3,9] With this in mind, we decided to investigate carboxylate-free reactions for the synthesis of Mn/Ln compounds and to use 2-(hydroxymethyl)pyridine (hmpH; see Scheme 1), whose deprotonated form is an excellent N,O-chelating and bridging ligand. In addition, hmpH belongs to

## Scheme 1. Structure of (2-Hydroxymethyl)pyridine
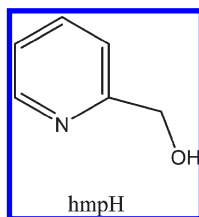


hmpH

the family of pyridine-based alkoxide ligands that often support ferromagnetic coupling between the metal atoms and have thus yielded several polynuclear 3d metal clusters with large $S$ values and SMM properties.[10] In 3d/4f chemistry, hmpH has been poorly investigated but yielded the interesting family of dinuclear $Cu^{II}Ln^{III}$ (Ln = Tb, Gd, La) compounds, the $Tb^{III}$ analogue of which possesses SMM behavior.[11] It has also been used in mixed 3d/3d chemistry,[12] but it has not been employed to date in mixed Mn/Ln or Mn/Y chemistry. We herein report a systematic investigation of the $Mn^{2+}/M^{3+}/hmpH/OH^-$ (M = Dy, Tb, Gd, Y) reaction system, which has yielded a family of tetranuclear $Mn^{III}_2M^{III}_2$ compounds with a planar-butterfly (or rhombus) core. The syntheses, structural, and detailed magnetic properties of these compounds are described.

## ■ EXPERIMENTAL SECTION

**Syntheses.** All manipulations were performed under aerobic conditions using materials (reagent grade) and solvents as received. **Caution!** *Although no such behavior was observed during the present work, perchlorate salts are potentially explosive; such compounds should be synthesized and used in small quantities and treated with utmost care at all times.*

**$[Mn_2Dy_2(OH)_2(NO_3)_4(hmp)_4(H_2O)_4](NO_3)_2$ (1).** *Method A.* To a stirred solution of hmpH (0.10 mL, 1.0 mmol) and NEt₃ (0.14 mL, 1.0 mmol) in MeCN (25 mL) was added solid Mn-$(ClO_4)_2 \cdot 6H_2O$ (0.36 g, 1.0 mmol), which caused a rapid color change to dark red. The mixture was stirred for a further 15 min, and then solid $Dy(NO_3)_3 \cdot 6H_2O$ (0.46 g, 1.0 mmol) was added under vigorous stirring. The solution was stirred for a further 1 h and filtered, and the filtrate was left undisturbed in an open flask. Slow evaporation of the solvent at room temperature gave orange crystals of $1 \cdot 2H_2O \cdot MeCN$, which were kept in mother liquor for X-ray analysis or collected by filtration and dried under vacuum for other solid-state studies. Yield: ~60%. Dried solid analyzed as $1 \cdot 3H_2O$. Anal. Calcd (Found): C, 20.60 (20.41); H, 2.88 (3.02); N, 10.01 (10.42). Selected IR data (KBr, cm⁻¹): 3390mb, 2966w, 2877w, 1627w, 1489m, 1384m, 1311m, 1078s, 1031s, 885m, 816m, 744s, 625m, 566w, 463w.

*Method B.* To a colorless stirred solution of hmpH (0.10 mL, 1.0 mmol) and NEt₃ (0.14 mL, 1.0 mmol) in MeCN (20 mL) was added a solution of $Mn(ClO_4)_2 \cdot 6H_2O$ (0.36 g, 1.0 mmol) and $Dy(NO_3)_3 \cdot 6H_2O$ (0.46 g, 1.0 mmol) in MeCN (5 mL). The mixture was stirred for 6 h, the resulting solution was filtered, and the filtrate was left undisturbed in an open flask. Slow evaporation of the solvent at room temperature gave orange crystals, which were collected by filtration, washed with Et₂O, and dried in vacuum. Yield: ~75%. The product was identified by IR spectral comparison and elemental analysis as identical with that from Method A. Anal. Calcd (Found) for $1 \cdot 3H_2O$: C, 20.60 (20.32); H, 2.88 (3.10); N, 10.01 (10.23).

**$[Mn_2Tb_2(OH)_2(NO_3)_4(hmp)_4(H_2O)_4](NO_3)_2$ (2).** This complex was prepared in the same manner (Method B) as complex 1 but using $Tb(NO_3)_3 \cdot 6H_2O$ (0.45 g, 1.0 mmol) in place of $Dy(NO_3)_3 \cdot 6H_2O$. After 3 days, X-ray-quality orange prismatic crystals of $2 \cdot 2H_2O \cdot MeCN$ were collected by filtration, washed with H₂O (3 mL), MeCN (2 × 5 mL), and Et₂O (2 × 5 mL), and dried under vacuum. Yield: ~60%.

## Table 1. Crystallographic Data for $1 \cdot 2H_2O \cdot MeCN$

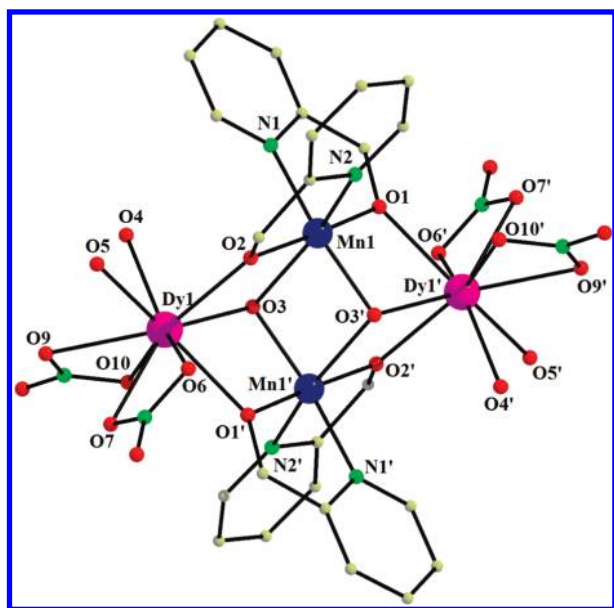| | |
|---|---|
| formula[a] | $C_{24}H_{38}Dy_2Mn_2N_{10}O_{30}$ |
| fw, g mol⁻¹ | 1381.52 |
| cryst syst | monoclinic |
| cpace group | $C2/c$ |
| $a$, Å | 19.515(4) |
| $b$, Å | 11.816(2) |
| $c$, Å | 11.816(2) |
| $\beta$, deg | 101.244(10) |
| $V$, Å³ | 4670.9 (5) |
| $Z$ | 4 |
| $T$, K | 100 (2) |
| radiation, Å [b] | 0.71073 |
| $\mu$ (mm⁻¹) | 3.795 |
| measured reflns | 46 836 |
| unique reflns ($R_{int}$) | 5372 (0.0498) |
| params refined | 317 |
| goodness-of-fit | 1.446 |
| $R_1$[c,d] | 0.0414 |
| $wR_2$[c,e] | 0.0952 |
| $(\Delta\rho)_{max}/(\Delta\rho)_{min}$ (e Å⁻³) | 1.349 /−1.381 |

[a] Excluding disordered MeCN. [b] Graphite monochromator. [c] $I > 2\sigma(I)$. [d] $R_1 = \Sigma(|F_o| - |F_c|)/\Sigma(|F_o|)$. [e] $wR_2 = [\Sigma w(F_o^2 - F_c^2)^2/\Sigma w(F_o^2)^2]^{1/2}$, $w = 1/[\sigma^2(F_o^2) + [(ap)^2 + bp]$, where $p = [F_o^2 + 2F_c^2]/3$.

Dried solid analyzed as $2 \cdot 2H_2O$. Anal. Calcd (Found): C, 20.97 (20.62); H, 2.79 (2.50); N, 10.19 (10.60). Selected IR data (KBr, cm⁻¹): 3413mb, 2960w, 2872w, 1631w, 1486m, 1384m, 1314m, 1079s, 1033s, 885m, 817m, 742s, 624m, 562w, 458w.

**$[Mn_2Gd_2(OH)_2(NO_3)_4(hmp)_4(H_2O)_4](NO_3)_2$ (3).** This complex was prepared in the same manner (Method B) as complex 1 but using $Gd(NO_3)_3 \cdot 6H_2O$ (0.45 g, 1.0 mmol) in place of $Dy(NO_3)_3 \cdot 6H_2O$. After 3 days, X-ray-quality orange prismatic crystals of $3 \cdot 2H_2O \cdot MeCN$ were collected by filtration, washed with H₂O (3 mL), MeCN (2 × 5 mL), and Et₂O (2 × 5 mL), and dried under vacuum. Yield: ~60%. Dried solid analyzed as $3 \cdot 2H_2O$. Anal. Calcd (Found): C, 21.03 (20.34); H, 2.79 (3.16); N, 10.22 (10.57). Selected IR data (KBr, cm⁻¹): 3385mb, 2974w, 2874w, 1629w, 1490m, 1386m, 1313m, 1080s, 1029s, 885m, 819m, 744s, 625m, 568w, 466w.

**$[Mn_2Y_2(OH)_2(NO_3)_4(hmp)_4(H_2O)_4](NO_3)_2$ (4).** This complex was prepared in the same manner (Method B) as complex 1 but using $Y(NO_3)_3 \cdot 6H_2O$ (0.38 g, 1.0 mmol) in place of $Dy(NO_3)_3 \cdot 6H_2O$. After 3 days, X-ray-quality orange prismatic crystals of $4 \cdot 2H_2O \cdot MeCN$ were collected by filtration, washed with H₂O (3 mL), MeCN (2 × 5 mL), and Et₂O (2 × 5 mL), and dried under vacuum. Yield: ~80%. Dried solid analyzed as $4 \cdot 3H_2O$. Anal. Calcd (Found): C, 23.02 (23.41); H, 3.22 (3.38); N, 11.18 (10.83). Selected IR data (KBr, cm⁻¹): 3394b, 2981w, 2879w, 1627w, 1494 m, 1386 m, 1314 m, 1080s, 1029s, 882 m, 818 m, 744s, 625 m, 571w, 464w.

**X-ray Crystallography.** Data were collected on a Siemens SMART PLATFORM equipped with a CCD area detector and a graphite monochromator utilizing Mo Kα radiation (λ = 0.71073 Å). Suitable crystals were attached to glass fibers using silicone grease and transferred to a goniostat where they were cooled to 173 K for data collection. Cell parameters for $1 \cdot 2H_2O \cdot MeCN$ were refined using up to 8192 reflections. A full sphere of data (1850 frames) was collected using the ω-scan method (0.3° frame width). The first 50 frames were remeasured at the end of data collection to monitor instrument and crystal stability (maximum correction on I was <1%). Absorption corrections by integration were applied based on measured indexed crystal faces. Crystal data and structure refinement parameters for $1 \cdot 2H_2O \cdot MeCN$ are listed in Table 1. An initial search of reciprocal

8960

dx.doi.org/10.1021/ic2011106 |*Inorg. Chem.* 2011, 50, 8959–8966

**Figure 1.** Structure of the cation of **1**. H atoms have been omitted for clarity. The Mn<sup>III</sup> Jahn−Teller elongation axes are N2−Mn1−O3 and its symmetry partner.

**Table 2. Selected Bond Distances (Å) and Angles (deg) for Complex 1**

| | | | |
|---|---|---|---|
| Mn1···Mn1′ | 3.250(4) | Dy1−O1′ | 2.342(4) |
| Dy1···Dy1′ | 6.198(4) | Mn1−O3′ | 1.952(4) |
| Mn1−Dy1 | 3.574(4) | Mn1−N1 | 2.043(5) |
| Dy1−O5 | 2.355(4) | Mn1−N2 | 2.206(5) |
| Dy1−O6 | 2.490(4) | Mn1−O1 | 1.877(4) |
| Dy1−O7 | 2.467(4) | Mn1−O2 | 1.892(4) |
| Dy1−O9 | 2.499(4) | Mn1−O3 | 2.249(4) |
| Dy1−O10 | 2.426(5) | | |
| Mn1−O3−Dy1 | 100.52(15) | Mn1−O2−Dy1 | 114.47(17) |
| Mn1−O3−Mn1′ | 101.09(17) | Mn1−O1−Dy1′ | 107.88(16) |

Only the full crystal structure of $1 \cdot 2H_2O \cdot MeCN$ was solved, because unit cell determinations, IR spectra, and elemental analyses indicated all the compounds to be isomorphous with isostructural cations. Formation of **1**−**4** is summarized in eq 1

$$2Mn^{2+} + 2M^{3+} + 4hmpH + 4NEt_3 + 4NO_3^- + 5H_2O$$
$$+ 0.5O_2 \xrightarrow{MeCN} [Mn_2M_2(OH)_2(hmp)_4(NO_3)_4(H_2O)_4]^{2+}$$
$$+ 4HNEt_3^+ \qquad (1)$$

where atmospheric $O_2$ is assumed to be the oxidizing agent to generate $Mn^{III}$ from $Mn^{II}$, facilitated by the basic conditions provided by $NEt_3$; in the absence of $NEt_3$, longer reaction times are required to get a significant violet coloration and the yields of the isolated products are much lower. On the other hand, greater than 2 equiv of $NEt_3$ does not alter the yield of product. **1**−**4** were also the only products we could isolate when other small changes to the reaction conditions were explored, such as to the reagent ratios, solvent, crystallization method, identity of the base, and presence of $NBu_4MnO_4$ to possibly access higher oxidation state products. The only effect was to affect the yield of **1**−**4** and lower slightly their crystallinity and/or purity.

**Description of Structure.** The structure of the $[Mn_2Dy_2(OH)_2(NO_3)_4(hmp)_4(H_2O)_4]^{2+}$ cation of **1** is shown in Figure 1. Selected interatomic distances and angles are listed in Table 2. Complex $1 \cdot 2H_2O \cdot MeCN$ crystallizes in the monoclinic space group $C2/c$ with the cation lying on an inversion center. The cation possesses a $[Mn^{III}_2Dy^{III}_2(\mu_3\text{-}OH)_2]^{10+}$ core consisting of a $Mn_2Dy_2$ planar-butterfly (or rhombus) with the Mn atoms at the body positions and each $Mn_2Dy$ triangular unit bridged by a $\mu^3$-$OH^-$ ion (O3) lying 0.971 Å above the $Mn_2Dy$ plane. The core is additionally monoatomically bridged at each MnDy edge by the alkoxide O atom of an $\eta^1:\eta^2:\mu$ hmp$^-$ group, which chelates a Mn atom. The structure of the core of **1** can alternatively be described as two face-sharing incomplete cubanes, i.e., with a metal atom missing from one vertex of each cubane. This defective-dicubane motif with a resulting $M_4$ rhombus is relatively common in both homo- and heterometallic cluster chemistry[16−18] and often possesses a crystallographic center of symmetry.

The Dy and Mn atoms are nine and six coordinate, respectively. The Mn oxidation states and the protonation level of $OH^-$ ions were suggested by the metric parameters and charge considerations and confirmed by bond-valence sum (BVS) calculations: the BVS values for Mn1 and O3 were 3.05 and 1.07, respectively, confirming a $Mn^{3+}$ and $OH^-$ situation. In addition, the $Mn^{III}$ atoms were clearly Jahn−Teller (JT) distorted, taking the form of an axial elongation of the

## ■ RESULTS AND DISCUSSION

**Syntheses.** Reaction of $Mn(ClO_4)_2 \cdot 6H_2O$ with equimolar amounts of hmpH, $NEt_3$, and $M(NO_3)_3 \cdot 6H_2O$ (M = Dy, **1**; Tb, **2**; Gd, **3**; Y, **4**) in MeCN afforded violet solutions from which were subsequently isolated $[Mn_2M_2(OH)_2(NO_3)_4(hmp)_4(H_2O)_4](NO_3)_2 \cdot 2H_2O \cdot MeCN$ in good yields (60−80%).

space for $X \cdot 2H_2O \cdot MeCN$ (X = **2**, **3**, and **4**) revealed monoclinic cells with dimensions identical with that of $1 \cdot 2H_2O \cdot MeCN$; thus, full solution of their crystal structures was not pursued.

The structure of $1 \cdot 2H_2O \cdot MeCN$ was solved by the direct methods in *SHELXTL6*[13] and refined on $F^2$ using full-matrix least-squares. The non-H atoms were treated anisotropically, whereas the H atoms were placed in calculated, ideal positions and refined as riding on their respective C atoms. The asymmetric unit consists of one-half a $Dy_2Mn_2$ cluster on an inversion center, a $NO_3^-$ anion, an ordered water solvate molecule, and an MeCN solvate molecule disordered against two partial $H_2O$ molecules; the latter were too disordered to be modeled properly; thus, the program SQUEEZE,[14] part of the PLATON package of crystallographic software, was used to calculate the solvent disorder area and remove its contribution to the overall data. The protons of the bridging $OH^-$ groups were freely refined; those of the $H_2O$ ligands were obtained from a difference Fourier map and refined as riding on their parent O atoms. A total of 317 parameters were refined in the final cycle of refinement using 5187 reflections with $I > 2\sigma(I)$ to yield $R_1$ and $wR_2$ of 4.14 and 9.52%, respectively.

**Other Studies.** Microanalyses (C, H, N) were performed by the in-house facilities of the Chemistry Department at the University of Florida. FTIR spectra (400−4000 cm$^{-1}$) were recorded on a Nicolet Nexus 670 spectrometer with the samples as KBr pellets. Variable-temperature dc and ac magnetic susceptibility data were collected using a Quantum Design MPMS-XL SQUID magnetometer equipped with a 7 T magnet and operating in the 1.8−300 K range. The samples were embedded in solid eicosane to prevent torquing. Pascal's constants[15] were used to estimate the diamagnetic corrections, which were subtracted from the experimental susceptibilities to give the molar paramagnetic susceptibilities ($\chi_M$).
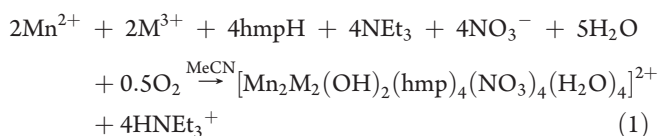
**Table 3. Hydrogen-Bonding Contacts in 1·2H$_2$O·MeCN**

| interaction | O···O (Å) | H···O (Å) | O−H···O (deg) |
|---|---|---|---|
| O5−H5···O12[a] | 2.644(4) | 1.77(1) | 172.0(1) |
| O12−H12···O6[a] | 2.963(4) | 2.02(1) | 179.1(1) |
| O3−H3···O13[b] | 2.745(4) | 2.02(1) | 156.0(1) |
| O4−H4···O15[b] | 2.793(4) | 1.70(1) | 156.1(1) |
| O5−H5···O15[b] | 2.825(4) | 2.15(1) | 151.5(1) |
| O4−H4···O14[b] | 2.734(4) | 1.88(1) | 161.7(1) |

[a] O12 belongs to the H$_2$O solvate molecule; [b] Atoms O13, O14, and O15 belong to the NO$_3^-$ counterion.



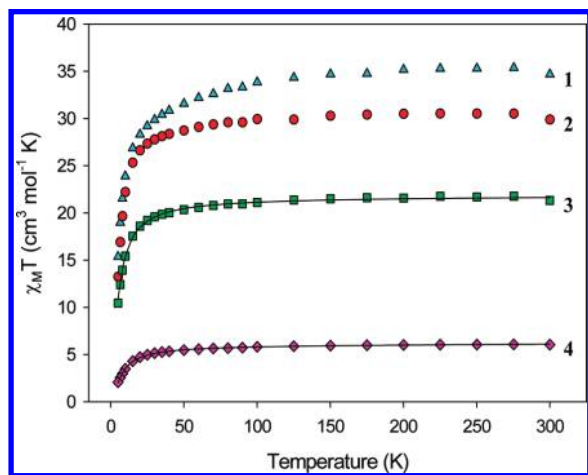**Figure 2.** $\chi_M T$ vs $T$ plots for 1·3H$_2$O, 2·2H$_2$O, 3·2H$_2$O, and 4·2H$_2$O in a 0.1 dc field. The solid lines are fits of the data to the corresponding theoretical expressions; see the text for the fit parameters.

N2−Mn1−O3 and its symmetry-related axis. Thus, Mn1−N2 (2.206(5) Å) and Mn1−O3 (2.249(4) Å) are distinctly longer than the other four bonds (1.877(4)−2.043(5) Å). The JT axes are aligned parallel as a result of the symmetry of the cation.

The crystal structure of 1·2H$_2$O·MeCN is stabilized by many O−H···O hydrogen bonds involving the hydroxo (O3), bound (O4, O5) and solvate (O12) H$_2$O groups, and NO$_3^-$ ligands as well as NO$_3^-$ counterions; these are listed in Table 3. The NO$_3^-$ counterions and the solvate water molecules form hydrogen-bonded bridges between adjacent Mn$_2$Dy$_2$ cations to give a network, but there are no hydrogen bonds directly between metal-bound H$_2$O or NO$_3^-$ ligands of one cation and metal-bound ligands of a neighboring cation. Thus, there might be exchange interactions between different Mn$_2$Dy$_2$ cations propagated by the hydrogen-bonding network, but they should nevertheless be weak.

Complexes 1−4 are new additions to the small family of Mn$_2$Ln$_2$ clusters possessing a rhombus or diamond-like core.[16,17] They are the first Mn$_2$Ln$_2$ compounds with hmp$^-$ ligands, and in fact, they are the first Mn/Ln and Mn/Y compounds of any type to be obtained with hmp$^-$ ligands. In addition, as stated earlier, previous Mn/Ln chemistry has been dominated by carboxylate-containing species, and 1−4 are the first noncarboxylate Mn$_2$Ln$_2$ compounds and rare examples of carboxylate-free Mn/Ln clusters of any type. It should be noted that the JT elongation axes in $\mu_3$-OH$^-$-bridged 1−4 contain the OH$^-$ groups, which is distinctly different from the one known $\mu_3$-O$^{2-}$-bridged Mn$_2$Gd$_2$



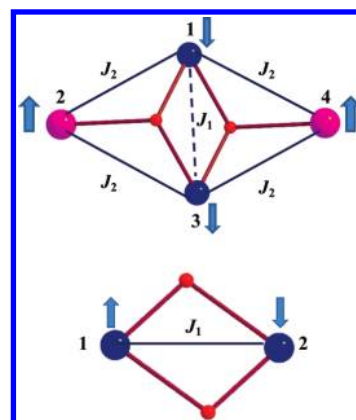**Figure 3.** (Top) Atom-labeling scheme and exchange interactions in the rhombus of 3·2H$_2$O, and the spin alignments in its $|S_T, S_A, S_B\rangle = |3, 4, 7\rangle$ ground state; (bottom) labeling scheme and spin alignments in the ground $S_T = 0$ state of 4·2H$_2$O.

complex where the JT axes avoid the Mn−O$^{2-}$ bonds,[17c] the usually observed situation. This obviously leads to a differing orientation of the Mn$^{III}$ d$_{z2}$ magnetic orbital.

**Magnetochemistry.** Solid-state, variable-temperature dc magnetic susceptibility ($\chi_M$) data were collected on vacuum-dried microcrystalline samples of complexes 1−4, suspended in eicosane to prevent torquing, in the 5.0−300 K range in a 0.1 T (1000 Oe) magnetic field; they are shown in Figure 2 as $\chi_M T$ vs $T$ plots. For 1·3H$_2$O, $\chi_M T$ steadily decreases with decreasing temperature from 34.68 cm$^3$ mol$^{-1}$ K at 300 K to 28.30 cm$^3$ mol$^{-1}$ K at 20 K and then more rapidly to 15.36 cm$^3$ mol$^{-1}$ K at 5.0 K. The $\chi_M T$ at 300 K is very close to the 34.34 cm$^3$ mol$^{-1}$ K calculated for two Mn$^{III}$ and two Dy$^{III}$ ($^6H_{15/2}$ free ion, $S = {}^5/_2$, $L = 5$, $g_J = 4/3$) noninteracting ions. For 2·2H$_2$O, $\chi_M T$ at 300 K is 29.89 cm$^3$ K mol$^{-1}$, essentially equal to the 29.64 cm$^3$ K mol$^{-1}$ calculated for two Mn$^{III}$ and two Tb$^{III}$ ($^7F_6$ free ion, $S = 3$, $L = 3$, $g_J = 3/2$) noninteracting ions. It slowly decreases with decreasing temperature down to 20 K and then more rapidly to 13.23 cm$^3$ K mol$^{-1}$ at 5.0 K. For 3·2H$_2$O, $\chi_M T$ steadily decreases with decreasing temperature from 21.32 cm$^3$ mol$^{-1}$ K at 300 K to 17.54 cm$^3$ mol$^{-1}$ K at 20 K and then more rapidly to 10.44 cm$^3$ mol$^{-1}$ K at 5.0 K. The 300 K value is essentially equal to the spin-only value of 21.75 cm$^3$ mol$^{-1}$ K for two Mn$^{III}$ and two Gd$^{III}$ noninteracting ions. For 4·3H$_2$O, the only paramagnetic ions are the two Mn$^{III}$ centers, since Y$^{III}$ is diamagnetic. $\chi_M T$ at 300 K is 6.04 cm$^3$ mol$^{-1}$ K, equal to the spin-only value of 6.00 cm$^3$ mol$^{-1}$ K for two Mn$^{III}$ noninteracting ions. It decreases only very slightly with decreasing temperature to 4.73 cm$^3$ mol$^{-1}$ K at 20 K and then more rapidly and is clearly heading for 0 cm$^3$ mol$^{-1}$ K at lower temperatures, indicating an $S = 0$ ground state. For all complexes, the $\chi_M T$ vs $T$ profiles are consistent with all intramolecular exchange interactions being very weak and being wholly or dominantly antiferromagnetic (AF) in nature.

The isotropic Heisenberg spin Hamiltonian describing the exchange interactions within an M$_4$ butterfly or rhombus topology is given by eq 2

$$\mathscr{H} = -2J_1\hat{S}_1\cdot\hat{S}_3 - 2J_2(\hat{S}_1\cdot\hat{S}_2 + \hat{S}_2\cdot\hat{S}_3 + \hat{S}_3\cdot\hat{S}_4 + \hat{S}_1\cdot\hat{S}_4) \qquad (2)$$

where $J_1$ denotes the Mn···Mn interaction between the 'body' Mn atoms and $J_2$ denotes the Mn···M (M = Dy, 1; Tb, 2; Gd, 3)

on the four edges (Figure 3, top). The long-range M···M interaction is assumed to be zero and is omitted. The corresponding eigenvalues are given by eq 3

$$E|S_T, S_A, S_B\rangle = -J_1[S_A(S_A + 1)] - J_2[S_T(S_T + 1) - S_A(S_A + 1) - S_B(S_B + 1)] \quad (3)$$

where $\hat{S}_A = \hat{S}_1 + \hat{S}_3$, $\hat{S}_B = \hat{S}_2 + \hat{S}_4$, $\hat{S}_T = \hat{S}_A + \hat{S}_B$, $S_T$ is the total spin of the molecule, and $E|S_T, S_A, S_B\rangle$ is the energy of state $S_T$ arising from particular $S_A$ and $S_B$ values.[10a,19] A theoretical expression for the molar paramagnetic susceptibility, $\chi_M T$, can be derived using the calculated $S_T$ states, their energies $E|S_T, S_A, S_B\rangle$, the van Vleck equation,[20] and assuming an isotropic $g$ tensor. This equation can then be used to fit the experimental $\chi_M T$ vs $T$ data in Figure 2 as a function of the two exchange parameters $J_1$ and $J_2$ and the $g$ factor.

For $1\cdot 3H_2O$ and $2\cdot 2H_2O$, the presence of strongly anisotropic $Dy^{III}$ and $Tb^{III}$ preclude use of the above approach because the isotropic spin Hamiltonian of eq 2 is not appropriate. In contrast, $3\cdot 2H_2O$ contains isotropic $Gd^{III}$. Thus, $S_1 = S_3 = 2$ and $S_2 = S_4 = 7/2$, and there are 160 $S_T$ states with values in the $S_T = 0-11$ range. A satisfactory fit was obtained with $J_1 = -0.16(2)$ $cm^{-1}$, $J_2 = -0.12(1)$ $cm^{-1}$, and $g = 2.0(1)$, with temperature-independent paramagnetism (TIP) held constant at $300 \times 10^{-6}$ $cm^3$ $mol^{-1}$; the fit is shown as the solid line in Figure 2. The exchange parameters are thus very weak, as expected when lanthanides are involved.[4,16,17] The obtained $J$ values identify the ground state to be $|S_T, S_A, S_B\rangle = |3, 4, 7\rangle$, with a low-lying $|4, 3, 7\rangle$ first excited state at 0.57 $cm^{-1}$ above the ground state. The individual spin alignments in the ground state are included in Figure 3(top).

Magnetization ($M$) vs dc field ($H$) data were collected for the $0.1-0.5$ and $1.8-2.5$ K ranges, and these are plotted in Figure S1, Supporting Information, as $M/N\mu_B$ vs $H/T$, where $N$ is Avogadro's number and $\mu_B$ is the Bohr magneton. The data were fit using the program MAGNET[21] as described in the Supporting Information, employing only data at very low fields to avoid problems from low-lying excited states. However, we still obtained a fit of only mediocre quality (solid lines in Figure S1, Supporting Information) with $S = 3$, $g = 2.0(1)$, and $D = -0.7(2)$ $cm^{-1}$. Nevertheless, the magnitude of the magnetization at a given field was in the region expected for an $S = 3$ state with $g \approx 2$, whereas $S = 2$ or 4 gave an unacceptably high or low $g$, respectively, lending some support to the conclusion from the above susceptibility fit that $3\cdot 2H_2O$ has an $S_T = 3$ ground state.

With the couplings being so weak, the accuracy of the obtained $J_1$ and $J_2$ values was a matter of concern in terms of both their exact magnitude and, more importantly, whether they really are both antiferromagnetic. Both weakly ferromagnetic (F)[16,22] and antiferromagnetic (AF)[23] Mn···Gd interactions are known, so the AF $J_2$ for $3\cdot 2H_2O$ is reasonable. Similarly, $Mn^{III}···Mn^{III}$ interactions can be both F and AF,[24] but the central $Mn^{III}···Mn^{III}$ interaction in $Mn_4$ rhombs with the JT axes involving the $\mu_3-OH^-$ or $OR^-$ groups are often ferromagnetic.[18] The possibility that one or other of $J_1$ and $J_2$ might in reality be ferromagnetic could thus not be discounted. Further, if they really are both AF, then the triangular subunits within the $Mn_2Gd_2$ core should lead to spin frustration effects (competing exchange interactions);[25] the determined $|3, 4, 7\rangle$ ground state corresponds to the individual spin alignments shown in Figure 3(top) and to those preferred by $J_2$; the parallel
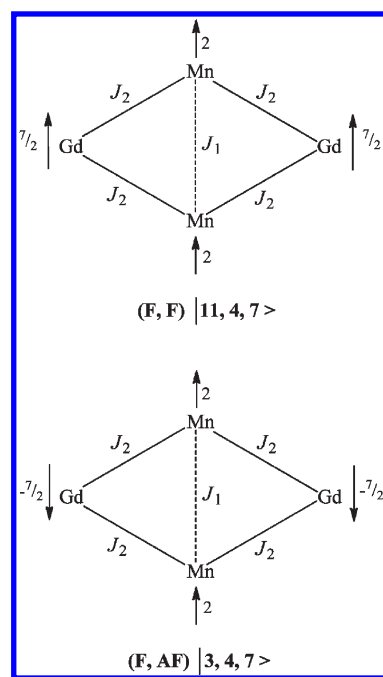


**Figure 4.** Spin alignments leading to the indicated $|S_T, S_A, S_B\rangle$ ground states for a $Mn^{III}_2Gd^{III}_2$ rhombus for (top) the (F, F) combination of $J_1$ and $J_2$ and (bottom) the (F, AF) combination; F = ferromagnetic, AF = antiferromagnetic.

alignment of $S_1$ and $S_3$ thus suggests complete frustration of $J_1$. It can be argued qualitatively that even though $J_1$ and $J_2$ are comparable in magnitude, there are four of the latter and only one of the former, which is thus overcome. Nevertheless, we decided to analyze the spin frustration patterns in this $Mn_2Gd_2$ core in a more quantitative manner and also to assess what to expect if one or both $J_1$ and $J_2$ are in fact F.

**Spin Frustration within the $Mn_2Gd_2$ Rhombus.** There are four possible combinations of sign for $J_1$ and $J_2$; in the format ($J_1$, $J_2$), these are (F, F), (F, AF), (AF, F), and (AF, AF). Two of these do not lead to spin frustration because $J_1$ and $J_2$ are not competing: (F, F) leads to a $|11, 4, 7\rangle$ ground state, the maximum $S_T$ possible for 3, for all relative magnitudes of $J_1$ and $J_2$, i.e., for all $J_2/J_1$ ratios. Similarly, (F, AF) leads to a $|3, 4, 7\rangle$ ground state for all $J_2/J_1$ ratios. These situations are shown in Figure 4. In contrast, the (AF, F) and (AF, AF) combinations lead to competition between $J_1$ and $J_2$, and the resulting spin alignments and ground state consequently become sensitive to the $J_2/J_1$ ratio. We calculated for both combinations the energies (normalized to $|J_1|$) of all the spin states of 3 as a function of $J_2/|J_1|$, and these are shown in Figure 5. Immediately apparent are the multiple ground states possible for each combination over only a narrow range of $J_2/|J_1|$. Once the latter exceeds $\sim 0.58$ for (AF, F) and $\sim -0.50$ for (AF, AF), the ground state is $|11, 4, 7\rangle$ and $|3, 4, 7\rangle$, respectively. Below these, however, the ground state is very sensitive to the precise $J_2/|J_1|$ value, spanning four different ground states as $J_2/|J_1|$ approaches zero. The limiting situation, i.e., $|J_2| \ll |J_1|$, corresponds to pairing up of the $Mn^{III}$ spins ($S_A = 0$), and the $Gd^{III}$ spins, which are assumed to be noninteracting in this model, form degenerate $S_B$ resultants spanning $S_B = S_T = 0-7$.

As described above, the fit of experimental $\chi_M T$ vs $T$ data for 3 gave $J_1 = -0.16(2)$ $cm^{-1}$ and $J_2 = -0.12(1)$ $cm^{-1}$, whose $J_2/|J_1|$
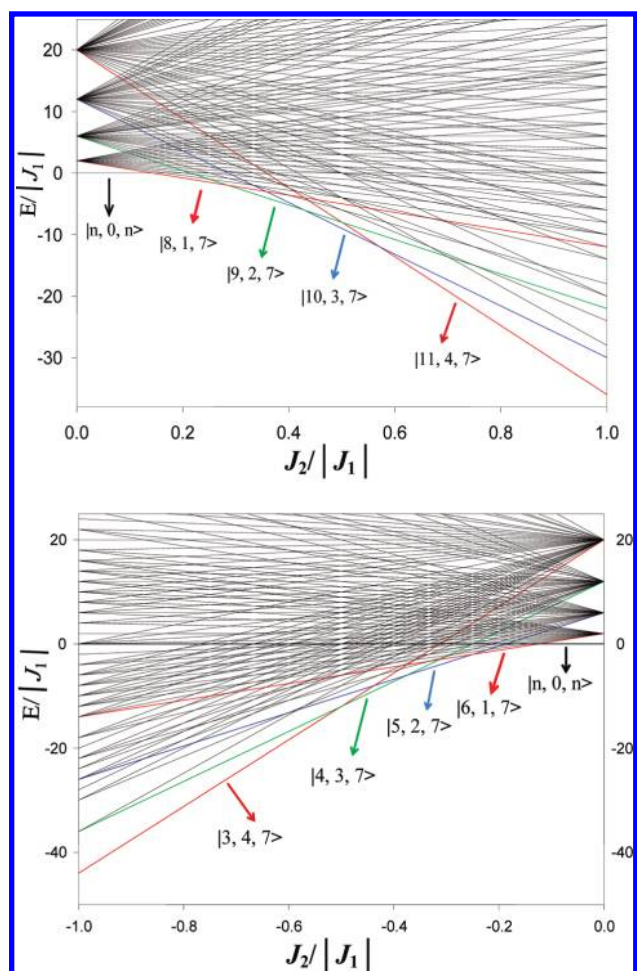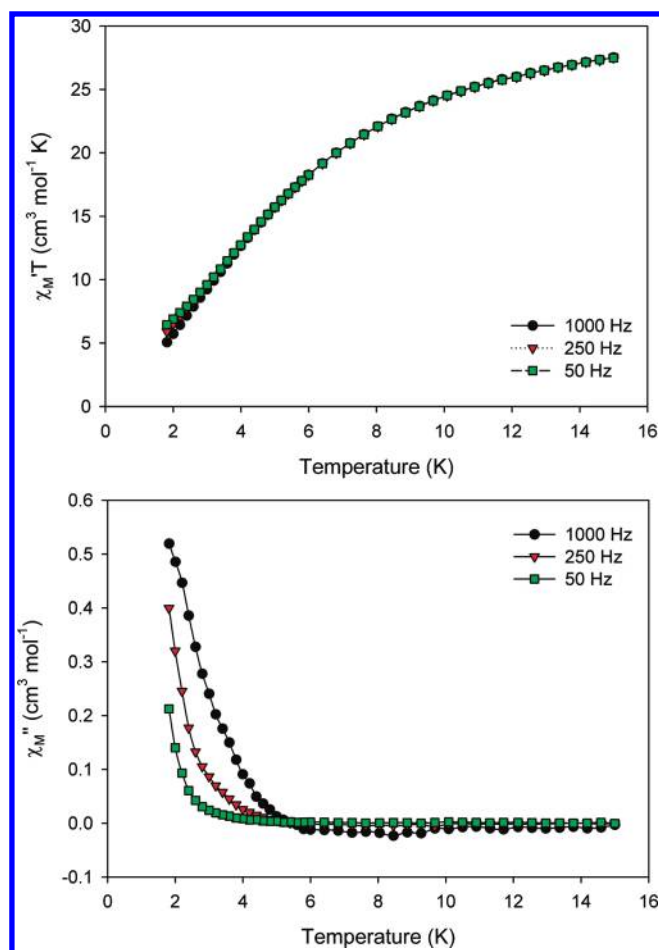
**Figure 5.** Variation of the spin-state energies of **3** with $J_2/|J_1|$ ratio for (top) the (AF, F) combination of $J_1$ and $J_2$ and (bottom) the (AF, AF) combination. Ground states are labeled as $|S_T, S_A, S_B\rangle$.

**Figure 6.** In-phase ac susceptibility ($\chi'_M$) signal, plotted as $\chi'_M T$ vs $T$ (top), and out-of-phase ($\chi''_M$) signal (bottom) for $\mathbf{1}\cdot 3H_2O$ in a 3.5 Oe field oscillating at the indicated frequencies.

ratio of $-0.75$ ($\pm 0.20$) puts it firmly in the $|3, 4, 7\rangle$ ground state region of Figure 5(bottom). Returning to the question of whether $J_1$ and/or $J_2$ might in reality be F, we see that the (AF, F) possibility (Figure 5, top) predicts much higher ground states than are consistent with the $\chi_M T$ vs $T$ profile of **3** in Figure 2. Similarly for the $S_T = 11$ ground state of (F, F) (Figure 4, top). However, the (F, AF) combination also predicts a $|3, 4, 7\rangle$ ground state, and it is in fact completely reasonable for $J_1$ to be F, as discussed earlier. We thus conclude that analyzing the spin frustration effects supports $J_2$ being AF but is much less useful in determining the sign of $J_1$. An additional, and preferably experimental, probe of $J_1$ was clearly needed, and this was in fact the primary reason we synthesized the isostructural $Mn_2Y_2$ complex $\mathbf{4}\cdot 3H_2O$, which only contains a $Mn^{III}Mn^{III}$ exchange interaction, $J_1$ (Figure 3, bottom). The spin Hamiltonian for a dinuclear complex is given by eq 4 and its eigenvalues by eq 5. For $\mathbf{4}\cdot 3H_2O$

$$\mathscr{H} = -2J_1(\hat{S}_1 \cdot \hat{S}_2) \tag{4}$$

$$E(S_T) = -J_1[S_T(S_T + 1)] \tag{5}$$

$S_1 = S_2 = 2$ and $S_T = 0-4$. The theoretical $\chi_M T$ vs $T$ expression[26] was used to fit the data (solid line in Figure 2), giving $J_1 = -0.75(3)$ cm$^{-1}$ and $g = 1.99(1)$, with TIP held constant at $300 \times 10^{-6}$ cm$^3$ mol$^{-1}$. The negative sign and small magnitude of $J_1$

thus support the $J_1$ of $\mathbf{3}\cdot 2H_2O$ also being weakly AF. The weak $J_1$ of **3** and **4** is in stark contrast to the much more strongly antiferromagnetic $Mn^{III}\cdots Mn^{III}$ coupling of $-31.45$ cm$^{-1}$ in $[Mn_2Gd_2O_2(O_2CBu^t)_8(HO_2CBu^t)_2(MeOH)_2].$[16] This is due to the two central $\mu_3$-$O^{2-}$ ions in this compound rather than $\mu_3$-$OH^-$ as in **3/4**. As a result, the $Mn^{III}$ JT axes are oriented differently in the former to avoid the $O^{2-}$ ions, and thus, the $d_{z^2}$ magnetic orbitals are also differently oriented. A major effect of the latter is to remove the ferromagnetic $d_{z^2}/d_{x^2-y^2}$ overlap between singly occupied and empty orbitals that is a major contributor to the weakly antiferromagnetic or ferromagnetic $Mn^{III}\cdots Mn^{III}$ coupling in **3/4** and homometallic $Mn_4$ rhombs, respectively.[10a,b,18]

**Alternating Current Magnetic Susceptibility Studies: Slow Relaxation in Complexes 1 and 2.** Alternating current susceptibility data below 15 K were collected in a 3.5 Oe ac field oscillating at 50−1000 Hz. The in-phase ($\chi'_M$, as $\chi'_M T$) and out-of-phase ($\chi''_M$) ac signals for $\mathbf{1}\cdot 3H_2O$ and $\mathbf{2}\cdot 2H_2O$ are shown in Figures 6 and 7, respectively. In both cases, $\chi'_M T$ decreases markedly with decreasing temperature but there is still significant paramagnetism remaining at 1.8 K. In addition, $\chi'_M T$ for $\mathbf{1}\cdot 3H_2O$ becomes slightly frequency dependent below ∼4 K, indicating the onset of slow magnetization relaxation vs the ac field, and indeed, there is a concomitant appearance of a frequency-dependent $\chi''_M$, which is strong ($\chi''_M / \chi'_M \approx 21\%$
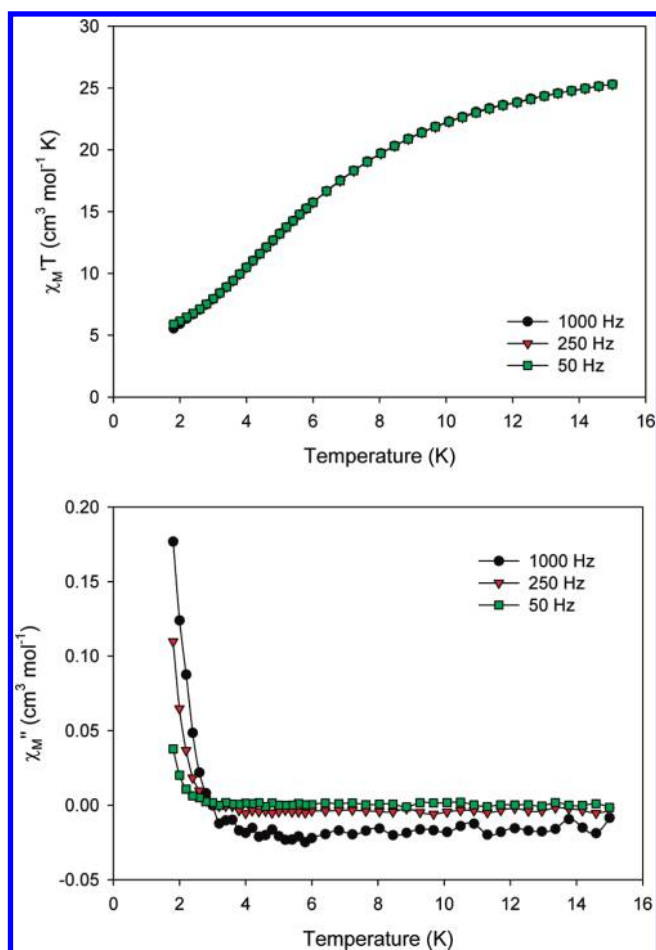
**Figure 7.** In-phase ac susceptibility ($\chi'_M$) signal, plotted as $\chi'_M T$ vs $T$ (top), and out-of-phase ($\chi''_M$) signal (bottom) for $2 \cdot 2H_2O$ in a 3.5 Oe field oscillating at the indicated frequencies.

at 1000 Hz at 1.8 K). For $2 \cdot 2H_2O$, there is just a trace of a frequency-dependent $\chi'_M T$ below 2 K but a clear frequency-dependent $\chi''_M$ signal, which is weaker ($\chi''_M/\chi'_M \approx 7\%$ at 1000 Hz at 1.8 K) than for $1 \cdot 3H_2O$, suggesting the peak is further below the 1.8 K operating limit of our SQUID magnetometer than the peak for $1 \cdot 3H_2O$. Nevertheless, the ac data indicate both $1 \cdot 3H_2O$ and $2 \cdot 2H_2O$ to be new examples of mixed 3d/4f single- molecule magnets, albeit with rather small relaxation barriers. Because there are now many SMMs known with such small barriers, we did not pursue single-crystal studies down to 0.04 K with a micro-SQUID to look for magnetization hysteresis.

The $\chi'_M T$ vs $T$ for $3 \cdot 2H_2O$ and $4 \cdot 3H_2O$ are shown in the Supporting Information (Figure S2). The former decreases markedly with decreasing temperature, consistent with depopulation of low-lying excited states, as suggested by the dc studies. Extrapolating the plot from $\sim 5$ K (to avoid weak intermolecular interactions that typically affect the lowest temperature data) gives a value of $\sim 5$ cm$^3$ K mol$^{-1}$ at 0 K, consistent with an $S = 3$ ground state with $g$ slightly <2, as expected for Mn$^{III}$. If the plot is extrapolated from 1.8 K, a value of $\sim 2$ cm$^3$ K mol$^{-1}$ is obtained, consistent with $S = 2$, but the above spin frustration analysis showed that $3 \cdot 2H_2O$ cannot have an $S = 2$ or 1 ground state, so this possibility is precluded. In any event, the crystal structure shows weak intermolecular H-bonded linkages (vide supra), so the presence of weak intermolecular exchange interactions is

expected. For $4 \cdot 3H_2O$, the $\chi'_M T$ vs $T$ plot is $\sim 1$ cm$^3$ K mol$^{-1}$ at 10 K and clearly is heading to 0 cm$^3$ K mol$^{-1}$ at 0 K, providing an independent confirmation that the coupling between the Mn$^{III}$ ions is antiferromagnetic, as deduced from the fit of the dc data. Both $3 \cdot 2H_2O$ and $4 \cdot 3H_2O$ exhibit no $\chi''_M$ signals down to 1.8 K (Figure S3, Supporting Information).

## ■ CONCLUSIONS

New examples of 3d/4f and 3d/4d tetranuclear clusters have been synthesized from the reactions of Mn$^{III}$ and Ln$^{III}$ or Y$^{III}$ sources with hmpH in the presence of a base. These products are new additions to the very small family of Mn$_2$M$_2$ clusters with a rhombus topology and a "planar-butterfly" or "incomplete dicubane" core structure. Complexes **1−3** are rare examples of carboxylate-free mixed Mn−Ln clusters. There is also only one previous example of such a compound (with any ligation) that has $\mu_3$-OH$^-$ ions rather than $\mu_3$-O$^{2-}$ or $\mu_3$-OR$^-$, where the latter is an alkoxide arm of a chelate. The magnetic study and detailed analysis of the spin frustration effects possible in Mn$^{III}_2$Gd$^{III}_2$ complex **3** together support the Mn$^{III}$Mn$^{III}$ and Mn$^{III}$Gd$^{III}$ exchange interactions to all be weakly AF. The spin frustration analysis of spin state energies as a function of the $J_2/J_1$ ratio has determined how the ground state changes as a function of the relative magnitude of the competing interactions, and we have shown how such an analysis can be useful in predicting what to expect in particular situations. It should be noted that when the absolute magnitude of the interactions is so weak, this of course introduces greater uncertainties and potential ambiguities, especially since other minor effects normally ignored, such as very weak intermolecular interactions, might not now be completely insignificant. Nevertheless, in the present case it seems that the combined data are all consistent with **3** having an $S_T = 3$ ground state, from $J_1$ and $J_2$ both being AF. In addition, the presence of the anisotropic Dy$^{III}$ and Tb$^{III}$ in **1** and **2** provides a sufficient barrier to yield the characteristic slow relaxation of SMMs, albeit with small barriers. Further work is in progress.

## ■ ASSOCIATED CONTENT

**ⓢ Supporting Information.** X-ray crystallographic data in CIF format for $1 \cdot 2H_2O \cdot MeCN$, and dc and ac magnetic data. This material is available free of charge via the Internet at http://pubs.acs.org.

## ■ AUTHOR INFORMATION

**Corresponding Author**
*Phone: 352-392-8314. Fax: 352-392-8757. E-mail: christou@chem.ufl.edu.

## ■ ACKNOWLEDGMENT

## ■ REFERENCES

(1) (a) Andruh, M.; Costes, J. P.; Diaz, C.; Gao, S. *Inorg. Chem.* **2009**, *48*, 3342. (b) Benelli, C.; Gatteschi, D. *Chem. Rev.* **2002**, *102*, 2369. (c) Winpenny, R. E. P. *Chem. Soc. Rev.* **1998**, *27*, 447. (d) Mori, F.; Nyui, T.; Ishida, T.; Nogami, T.; Choi, K. Y.; Nojiri, H. *J. Am. Chem. Soc.* **2003**, *125*, 8694. (e) Ishikawa, N. *Polyhedron* **2007**, *26*, 2147.

(2) Osa, S.; Kido, T.; Matsumoto, N.; Re, N.; Pochaba, A.; Mrozinski, J. *J. Am. Chem. Soc.* **2004**, *126*, 420.

(3) Zaleski, M; Depperman, E. C.; Kampf, J. W.; Kirk, M.-L.; Pecoraro, V. L. *Angew. Chem., Int. Ed.* **2004**, *43*, 3912.

(4) Mishra, A.; Wernsdorfer, W.; Abboud, K. A.; Christou, G. *J. Am. Chem. Soc.* **2004**, *126*, 15648.

(5) (a) Friedman, J. R.; Sarachik, M. P.; Tejada, J.; Ziolo, R. *Phys. Rev. Lett.* **1996**, *76*, 3830. (b) Thomas, L.; Lionti, L.; Ballou, R.; Gatteschi, D.; Sessoli, R.; Barbara, B. *Nature* **1996**, *383*, 145. (c) Aubin, S. M. J.; Gilley, N. R.; Pardi, L.; Krzystek, J.; Wemple, M. W.; Brunel, L.-C.; Maple, M. B.; Christou, G.; Hendrickson, D. N. *J. Am. Chem. Soc.* **1998**, *120*, 4991. (d) Barbara, B.; Wernsdorfer, W.; Sampaio, L. C.; Caneschi, J. G.; Hasselbach, K.; Benoit, A.; Thomas, L. *Magn. Magn. Mater.* **1995**, *140*, 1825.

(6) (a) Papatriantafyllopoulou, C.; Wernsdorfer, W.; Abboud, K. A.; Christou, G. *Inorg. Chem.* **2011**, *50*, 421. (b) Stamatatos, T. C.; Teat, S. J.; Wernsdorfer, W.; Christou, G. *Angew. Chem., Int. Ed.* **2009**, *48*, 521.

(7) (a) Mereacre, V.; Ako, A. M.; Clerac, R.; Wernsdorfer, W.; Filoti, G.; Bartolome, J.; Anson, C. E.; Powell, A. K. *J. Am. Chem. Soc.* **2007**, *129*, 9248. (b) Mereacre, V.; Ako, A. M.; Clerac, R.; Wernsdorfer, W.; Hewitt, I. J.; Anson, C. E.; Powell, A. K. *Chem.—Eur. J.* **2008**, *14*, 3577. (c) Langley, S.; Moubaraki, B.; Murray, K. S. *Dalton Trans.* **2010**, *39*, 5066.

(8) (a) Panagiotopoulos, A.; Zafiropoulos, Th. F.; Perlepes, S. P.; Bakalbassis, E.; Masson-Ramade, I.; Kahn, O.; Terzis, A.; Raptopoulou, C. P. *Inorg. Chem.* **1995**, *34*, 4918. (b) Kajiwara, T.; Takahashi, K.; Hiraizumi, T.; Takaishia, S.; Yamashita, M. *CrystEngComm* **2009**, *11*, 2110. (c) Rinck, J.; Novitchi, G.; Van den Heuvel, W.; Ungur, L.; Lan, Y.; Wernsdorfer, W.; Anson, C. E.; Chibotaru, L. F.; Powell, A. K. *Angew. Chem., Int. Ed.* **2010**, *49*, 7583.

(9) (a) Bi, Y.; Wang, X.-T.; Wang, B.-W.; Liao, W.; Wang, X.; Zhang, H.; Gao, S.; Li, D. *Dalton Trans.* **2009**, 2250. (b) Karotsis, G.; Evangelisti, M.; Dalgarno, S. J.; Brechin, E. K. *Angew. Chem., Int. Ed.* **2009**, *48*, 9928.

(10) (a) Yoo, J.; Yamaguchi, A.; Nakano, M.; Krzystek, J.; Streib, W. E.; Brunel, L.-C.; Ishimoto, H.; Christou, G.; Hendrickson, D. N. *Inorg. Chem.* **2001**, *40*, 4604. (b) Yang, E.-Ch; Harden, N.; Wernsdorfer, W.; Zakharov, L.; Brechin, E. K.; Rheingold, A. L.; Christou, G.; Hendrickson, D. N. *Polyhedron* **2003**, *22*, 1857. (c) Harden, N. C.; Bolcar, M. A.; Wernsdorfer, W.; Abboud, K. A.; Streib, W. E.; Christou, G. *Inorg. Chem.* **2003**, *42*, 7067. (d) Christmas, C. A.; Tsai, H.-L.; Pardi, L.; Kesselman, J. M.; Gantzel, P. K.; Chadha, R. K.; Gatteschi, D.; Harvey, D. F.; Hendrickson, D. N. *J. Am. Chem. Soc.* **1993**, *115*, 12483. (e) Stamatatos, T. C.; Abboud, K. A.; Wernsdorfer, W.; Christou, G. *Angew. Chem., Int. Ed.* **2007**, *46*, 884. (f) Stamatatos, T. C.; Abboud, K. A.; Wernsdorfer, W.; Christou, G. *Angew. Chem., Int. Ed.* **2006**, *45*, 4134. (g) Stamatatos, T. C.; Abboud, K. A.; Wernsdorfer, W.; Christou, G. *Polyhedron* **2007**, *26*, 2042. (h) Stamatatos, T. C.; Poole, K. M.; Abboud, K. A.; Wernsdorfer, W.; O'Brien, T. A.; Christou, G. *Inorg. Chem.* **2008**, *47*, 5006. (i) Murugesu, M.; Takahashi, S.; Wilson, A.; Abboud, K. A.; Wernsdorfer, W.; Hill, S.; Christou, G. *Inorg. Chem.* **2008**, *47*, 4095.

(11) He, F.; Tong, M.-L.; Chen, X.-M. *Inorg. Chem.* **2005**, *44*, 8285.

(12) (a) Vallina, A. T.; Lecren, L.; Li, Y.-G.; Roubeau, O.; Clérac, R. *Z. Anorg. Allg. Chem.* **2007**, *633*, 2400. (b) Feng, P. L.; Beedle, C. C.; Wernsdorfer, W.; Koo, C.; Nakano, M.; Hill, S.; Hendrickson, D. N. *Inorg. Chem.* **2007**, *46*, 8126. (c) Feng, P. L.; Beedle, C. C.; Koo, C.; Wernsdorfer, W.; Nakano, M.; Hill, S.; Hendrickson, D. N. *Inorg. Chem.* **2008**, *47*, 3188.

(13) *SHELXTL6*; Bruker-AXS: Madison, WI, 2000.

(14) Van der Sluis, P.; Spek, A. L. *Acta Crystallogr., Sect. A* **1990**, *A46*, 194.

(15) Weast, R. C. *CRC Handbook of Chemistry and Physics*; CRC Press, Inc.: Boca Raton, FL, 1984.

(16) Benelli, C.; Murrie, M.; Parsons, S.; Winpenny, R. E. P. *J. Chem. Soc., Dalton Trans.* **1999**, 4125.

(17) (a) Mishra, A.; Wernsdorfer, W.; Parsons, S.; Christou, G.; Brechin, E. K. *Chem Commun.* **2005**, 2086. (b) Murugesu, M.; Mishra, A.; Wernsdorfer, W.; Abboud, K. A.; Christou, G. *Polyhedron* **2006**,

25, 613. (c) Mukherjee, S.; Daniels, M. R.; Bagai, R.; Abboud, K. A.; Christou, G.; Lampropoulos, C. *Polyhedron* **2010**, *29*, 54.

(18) Roubeau, O.; Clérac, R. *Eur. J. Inorg. Chem.* **2008**, 4325 and references therein.

(19) Kambe, K. *J. Phys. Soc. Jpn.* **1950**, *S*, 48.

(20) Van Vleck, J. H. *The Theory of Electric and Magnetic Susceptibilities*; Oxford Press: London, 1932.

(21) Davidson, E. R. *Magnet*; Indiana University: Bloomington, IN, 1999.

(22) Lampropoulos, C.; Stamatatos, T. C.; Abboud, K. A.; Christou, G. *Inorg. Chem.* **2009**, *48*, 29.

(23) Mereacre, V.; Lan, Y.; Clérac, R.; Ako, A. M.; Hewitt, I. J.; Wernsdorfer, W.; Buth, G.; Anson, C. E.; Powell, A. K. *Inorg. Chem.* **2010**, *49*, 5293.

(24) Stamatatos, T. C.; Christou, G. *Philos. Trans. R. Soc. A* **2008**, *366*, 113.

(25) (a) Libby, E.; McCusker, J. K.; Schmitt, E. A.; Folting, K.; Hendrickson, D. N.; Christou, G. *Inorg. Chem.* **1991**, *30*, 3486. (b) Kahn, O. *Chem. Phys. Lett.* **1997**, *265*, 109.

(26) O' Connor, C. J. *Prog. Inorg. Chem.* **1982**, *29*, 203.

8966

dx.doi.org/10.1021/ic2011106 |*Inorg. Chem.* 2011, 50, 8959–8966